

Dual Incorporation of Photoaffinity Ligands on Dopamine Transporters Implicates Proximity of Labeled Domains

ROXANNE A. VAUGHAN, JON D. GAFFANEY, JOHN R. LEVER, MAARTEN E. A. REITH, and ALOKE K. DUTTA

Department of Biochemistry and Molecular Biology, University of North Dakota School of Medicine and Health Sciences, Grand Forks, North Dakota (R.A.V., J.D.G.); Department of Environmental Health Sciences, Johns Hopkins University School of Hygiene and Public Health, Baltimore, Maryland (J.R.L.); Department of Biomedical and Therapeutic Science, University of Illinois, Peoria, Illinois (M.E.A.R.); and Department of Pharmaceutical Sciences, Wayne State University, Detroit, Michigan (A.K.D.)

Received September 26, 2000; accepted February 1, 2001

This paper is available online at <http://molpharm.aspetjournals.org>

ABSTRACT

We have recently developed novel high-affinity blockers for the dopamine transporter (DAT) by carrying out structure-activity studies of GBR 12909 molecule piperidine analogs. To investigate the molecular basis of binding of these compounds in comparison to known sites of action of GBR 12909, cocaine, and benztropine analogs, we developed a piperidine-based photoaffinity label [¹²⁵I]4-[2-(diphenylmethoxy)ethyl]-1-[(4-azido-3-iodophenyl)methyl]-piperidine [¹²⁵I]AD-96-129, and used proteolysis and epitope-specific immunoprecipitation to identify the protein domains that interact with the ligand. [¹²⁵I]AD-96-129 became incorporated into two different regions of the DAT primary sequence, an N-terminal site containing transmembrane domains (TMs) 1 to 2, and a second site containing TMs 4 to 6. Both of these regions have been identified previously as sites involved in the binding of other DAT photoaffinity labels.

However, in contrast to the previously characterized ligands that showed nearly complete specificity in their binding site incorporation, [¹²⁵I]AD-96-129 became incorporated into both sites at comparable levels. These results suggest that the two domains may be in close three-dimensional proximity and contribute to binding of multiple uptake blockers. We also found that DATs labeled with [¹²⁵I]AD-96-129 or other photoaffinity labels displayed distinctive sensitivities to proteolysis of a site in the second extracellular loop, with protease resistance related to the extent of ligand incorporation in the TM4 to 6 region. These differences in protease sensitivity may indicate the relative proximity of the ligands to the protease site or reflect antagonist-induced conformational changes in the loop related to transport inhibition.

The dopamine transporter (DAT) is a neuronal protein that clears dopamine from the synaptic space, controlling synaptic dopamine concentrations and regulating dopamine availability for pre- and postsynaptic receptors. DAT is a major target for psychostimulant drugs such as cocaine (Kuhar et al., 1991), and for neurotoxins such as 1-methyl-4-phenyl-1,2,3,6-tetrahydropyridine (Kinemuchi et al., 1987). DAT and related neurotransmitter transporters are integral membrane proteins believed to consist of 12 transmembrane spanning domains (TMs), extracellularly oriented glycosylation sites, and intracellularly oriented N and C termini (Povlock and Amara, 1997). Although some of the structural aspects of these proteins predicted from primary sequence have been

experimentally verified, many important details of structure, including relative proximity of transmembrane spanning helices and identification of substrate and antagonist active sites, remain to be elucidated.

Although the binding properties of cocaine and other structurally diverse dopamine uptake blockers have been extensively characterized (Mash and Staley, 1997), it is not clear how they bind to DAT or how this results in transport inhibition. Different ligands could bind to the same site, to different sites, or to overlapping but nonidentical sites. Some studies compatible with the latter have suggested that slight differences in protein-ligand interactions may lead to subtle differences in transporter function. For instance, cocaine and GBR analogs display dissimilarities in their in vitro binding characteristics (Madras et al., 1989; Pristupa et al., 1994) and produce different behavioral profiles in vivo (Rothman et al., 1992; Izenwasser et al., 1994). Specific residues and domains of DAT are also thought to contribute differentially to

This work was supported by ND EPSCoR and National Institutes of Health Grants DA13147 (R.A.V.), DA08647 (A.K.D.), and DA08870 (J.R.L.). We thank Vickie Swift, University of North Dakota Graphics Department, for providing artwork.

ABBREVIATIONS: DAT, dopamine transporter; TM, transmembrane domain; GBR, GBR 12909 ([2-(diphenylmethoxy)ethyl]-4-(3-phenylpropyl)piperazine); [¹²⁵I]DEEP, 1-[2-(diphenylmethoxy)ethyl]-4-[2-(4-azido-3-iodophenyl)ethyl]piperazine; [¹²⁵I]GA II 34, 4-(4'-azido-3'-iodophenyl)-*n*-butyl 3- α -[bis(4'-fluorophenyl)methoxy]tropane; [¹²⁵I]RTI 82, 3 β -(*p*-chlorophenyl)tropane-2 β -carboxylic acid, 4'-azido-3'-iodophenylethyl ester; SERT, serotonin transporter; VMAT, vesicle monoamine transporter; [¹²⁵I]AD-96-129, 4-[2-(diphenylmethoxy)ethyl]-1-[(4-azido-3-iodophenyl)methyl]-piperidine; PAGE, polyacrylamide gel electrophoresis; NET, norepinephrine transporter; EL, extracellular loop.

transport and ligand binding (Kitayama et al., 1992; Buck and Amara, 1994, 1995; Giros et al., 1994).

Using irreversible DAT antagonists we have directly identified distinct sites of protein-ligand interactions. [125 I]DEEP, a GBR-based photoaffinity ligand, and [125 I]GA-II-34, a benzotropine derivative, become incorporated in TMs 1 to 2, whereas [125 I]RTI-82, a cocaine analog, becomes incorporated in a region of the protein containing TMs 4 to 7 (Vaughan 1995; Vaughan and Kuhar 1996; Vaughan et al., 1999). Thus, although the tropane ring is an essential component of the cocaine pharmacophore (Carroll et al., 1992), it is insufficient to produce identical targeting of [125 I]GA-II-34 and [125 I]RTI-82. However, we were unable to determine the basis for this differential ligand incorporation or the functional and structural relationship between the two protein domains.

The present study examines a newly developed ligand generated from GBR structures (Dutta et al., 1996, 1997, 1998a,b). Altering the GBR piperazine ring into a piperidine ring, in addition to other modifications (Fig. 1), produced high-affinity DAT ligands that showed striking increases in DAT/SERT selectivity (Dutta et al., 1997, 1998a,b). To investigate the molecular basis of binding of these compounds we developed a corresponding photoaffinity derivative, 4-[2-(diphenylmethoxy)ethyl]-1-[(4-azidophenyl)methyl]-piperidine ([125 I]AD-96-129) (Dutta et al., 2001b), and mapped its photoincorporation sites in comparison to the known labeling patterns of [125 I]DEEP, [125 I]RTI-82, and [125 I]GA-II-34. Although [125 I]AD-96-129 interacts with the same regions as the other photoaffinity labels, it does so with a two-site pattern of incorporation not previously observed for DAT. This strongly implicates the three-dimensional proximity of the labeled domains and provides one of the first indications of the three-dimensional nature of DAT antagonist binding sites.

Experimental Procedures

Photoaffinity Labeling. [125 I]DEEP, [125 I]RTI 82, and [125 I]AD-96-129 (specific activity 1600–2000 Ci/mmol) were synthesized as described previously (Lever et al., 1993; Dutta et al., 2001b) and used to label rat striatal membranes (Vaughan and Kuhar, 1996). Striatal

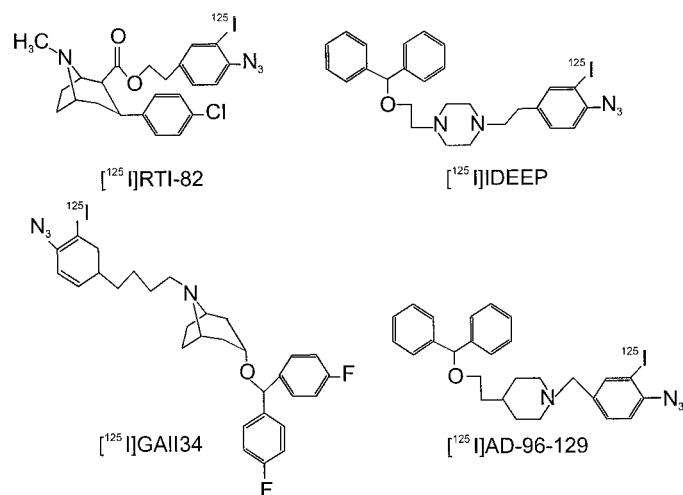


Fig. 1. DAT photoaffinity labels whose sites of incorporation have been identified. The structures show the positions of the azido (N_3) moiety, through which the ligands become covalently attached to the protein.

tissue was homogenized with a Polytron homogenizer in sucrose-phosphate buffer (10 mM sodium phosphate plus 0.32 M sucrose, pH 7.4), and homogenates were centrifuged at 12,000g for 12 min. The resulting membranes were resuspended at 15 mg/ml original wet weight in the same buffer, and radioligand was added to a final concentration of 5 nM. After a 60-min incubation on ice, ligand was covalently incorporated into DAT by irradiating the sample with ultraviolet light for 45 s, and membranes were washed with buffer. The photolabeled membranes were either solubilized with SDS-PAGE sample buffer (62.5 mM Tris-HCl, pH 6.8, 2% SDS, 10% glycerol, and 5 mM dithiothreitol) followed by electrophoresis, autoradiography, and electroelution of DAT (Vaughan, 1995), or were suspended in 50 mM Tris-HCl, pH 8.0, for in situ proteolysis and immunoprecipitation (Vaughan and Kuhar, 1996). Rats were housed and maintained in accordance with guidelines established by the University of North Dakota Animal Care and Use Committee and the National Institutes of Health.

Proteolysis. Gel purification and electroelution of photolabeled DAT were performed for experiments in which it was desired to remove other radiolabeled proteins present in striatal membranes. Proteolysis of these samples allows visualization of all DAT photolabeled fragments, regardless of their ability to be immunoprecipitated. For these experiments (Fig. 2), 25 μl of electroeluted sample was incubated for 1 h at 22°C with 25 μl of trypsin prepared in 50 mM Tris-HCl, pH 8.0. Reactions were stopped by adding 1 mg/ml trypsin inhibitor and 100 μl of SDS-PAGE sample buffer, followed by electrophoresis and autoradiography on 13% SDS-PAGE gels. For in situ proteolysis of membrane suspensions (Figs. 3–5 and 7), 25 μl of photolabeled membranes was incubated for 10 min at 22°C with 25 μl of trypsin in 50 mM Tris-HCl, pH 8.0. Reactions were stopped by adding 1 mg/ml trypsin inhibitor and centrifugation at 11,000g for 9 min. Supernatants were removed, and membranes were solubilized with 0.5% SDS followed by immunoprecipitation. Fragments generated from native and denatured protein correspond to comparable domains based on their similar immunoprecipitation properties (Vaughan, 1995; Vaughan and Kuhar, 1996). All experiments were repeated two to five times with similar results.

Immunoprecipitation, Electrophoresis, and Autoradiography. Epitope-specific immunoprecipitation of DAT and DAT fragments was performed as previously described using antiserum 16

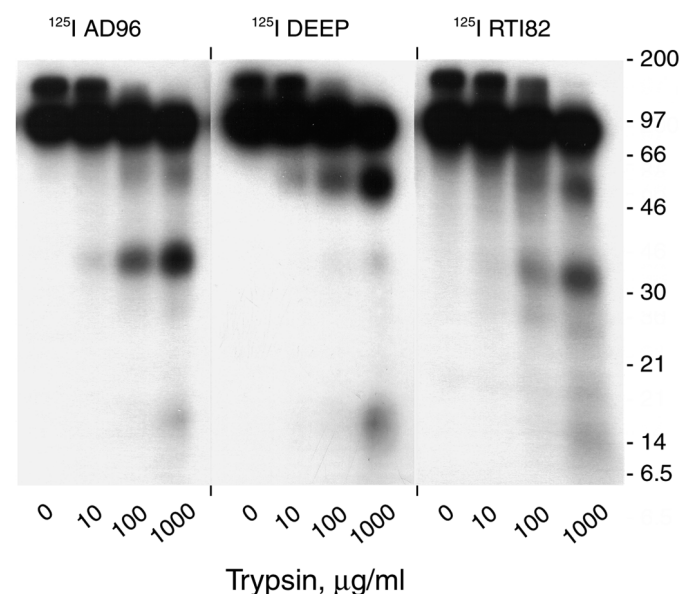


Fig. 2. Peptide maps of DATs labeled with [125 I]AD-96-129, [125 I]DEEP, and [125 I]RTI 82. Gel-purified photoaffinity-labeled DATs were treated with the indicated concentrations of trypsin, followed by electrophoresis on 13% SDS polyacrylamide gels and autoradiography. Molecular mass standards for all gels are shown in kilodaltons.

generated against amino acids 42 to 59 or antiserum 5 generated against amino acids 225 to 238 (Vaughan, 1995; Vaughan and Kuhar, 1996). For peptide competition experiments, diluted antisera were preincubated with 50 $\mu\text{g}/\text{ml}$ peptide 16 or peptide 5 before addition of DAT samples. Precipitated samples were electrophoresed on 13% or 9 to 16% SDS-polyacrylamide gels, and subjected to autoradiography using Kodak BioMax MS film for 1 to 4 days or PhosphorImager analysis and quantitation using a Molecular Dynamics PhosphorImager and ImageQuant software. The migration of DAT and DAT fragments relative to molecular mass standards varies slightly depending on the gel system used (Vaughan, 1995) and, in this study, are referred to by the previously ascribed values, which reflect our most accurate estimates of their masses (Vaughan, 1995; Vaughan and Kuhar, 1996). Photolabeling, proteolysis, and immunoprecipitation of DATs labeled with each ligand were done exactly in parallel. Autoradiographic exposures were adjusted to equalize band intensities between photolabeled samples, which differed due to differences in ligand affinities and specific activities.

Materials. Tosyl-phenylalanyl-chloromethyl ketone-treated trypsin and trypsin inhibitor were from Worthington Biochemical Corporation (Lakewood, NJ), protein A Sepharose CL4B and High and Low Range Rainbow Molecular Weight Markers were from Amersham Pharmacia Biotech (Piscataway, NJ), and other reagents were from Fischer Scientific (Pittsburgh, PA) or Sigma Chemical (St. Louis, MO).

Results

Peptide Maps of DATs Labeled with [^{125}I]AD-96-129, [^{125}I]DEEP, and [^{125}I]RTI 82. The overall peptide mapping pattern of DATs labeled with [^{125}I]AD-96-129 was first examined in comparison to the well characterized patterns generated from DATs labeled with [^{125}I]DEEP and [^{125}I]RTI 82 (Fig. 2). This experiment was performed using preparations of gel-purified DAT in which DAT is the only radiolabeled protein in the sample, thus all fragments shown derive from DAT and can be visualized regardless of their ability to be immunoprecipitated. The mapping pattern of DATs labeled with [^{125}I]DEEP was consistent with previous studies showing major fragments of about 45 and 14 kDa that originate from N-terminal regions of the protein, and a lightly labeled fragment at about 32 kDa that originates from C-terminal regions. Proteolysis of [^{125}I]RTI 82-labeled DATs also produced previously described fragments of about 32 and 16 kDa that originate from the C-terminal and central regions of the protein and a larger fragment at ~ 50 kDa distinct from the [^{125}I]DEEP-labeled 45-kDa fragment (see below). The relationship of these fragments to the primary sequence is described more thoroughly below and is summarized in Fig. 6. The peptide map of [^{125}I]AD-96-129-labeled DATs contained major photolabeled fragments evident at 45 and 32 kDa, as well as smaller fragments in the 14- to 16-kDa range. Since the different fragments generated from DATs labeled with [^{125}I]DEEP or [^{125}I]RTI 82 result from incorporation of the ligands in different regions of the DAT primary sequence, the pattern of fragments obtained from [^{125}I]AD-96-129 indicated the possibility that the ligand was incorporated into different protein domains. The substantial levels of radioactivity present in the fragments indicate that they represent major sites of photolabeling, but do not exclude the possibility that potential fragments derived from labeling of distinct sites might be lost due to small size.

Epitope-Specific Immunoprecipitation of Photolabeled Fragments. To identify the incorporation site(s) of

^{125}I -AD-96-129 in the DAT primary sequence, we treated labeled membrane suspensions with trypsin, removed the protease by washing the membranes, and immunoprecipitated the solubilized membranes with DAT antiserum 16, which recognizes amino acids 42 to 59 in the N-terminal tail just before TM1, or antiserum 5, which recognizes amino acids 225 to 238 in EL2 just before TM4 (Fig. 3). Proteolysis and immunoprecipitation were performed in parallel with samples labeled with [^{125}I]DEEP and [^{125}I]RTI 82 to serve as controls and points of reference. For both the [^{125}I]AD-96-129- and [^{125}I]DEEP-labeled samples (Fig. 3, left), serum 16 precipitated full-length DATs that migrate at about 80 kDa and tryptic fragments of approximately 45 and 14 kDa (Fig. 3, left arrows). Precipitation of the same [^{125}I]AD-96-129-labeled sample with antiserum 5 (Fig. 3, right) resulted in the extraction of full-length protein and 32- and 16-kDa fragments that comigrated with [^{125}I]RTI 82-labeled fragments (Fig. 3, right arrows), and a slight amount of the 50-kDa fragment. The 50-kDa [^{125}I]RTI 82-labeled fragment is not the same as the 45-kDa fragment labeled with [^{125}I]DEEP because it does not immunoprecipitate with serum 16 (data not shown). Some nonspecific [^{125}I]AD-96-129-labeled bands (e.g., at 32 kDa) were present at times but do not seem to be derived from DAT because they were present in nonprotease-treated samples, and may result from residual carryover of a prominent 32-kDa protein present in the starting sample (Fig. 5). The fragments identified in these experiments are retained in membranes after proteolytic treatment, indicating that they contain transmembrane spanning structure and that the binding of these ligands is closely associated with TM helices.

The specificity of the immunoprecipitation of photolabeled fragments was verified by competition with the immunizing peptide (Fig. 4). In Fig. 4, left, tryptic digests of DATs labeled with [^{125}I]AD-96-129 or [^{125}I]DEEP and precipitated with serum 16 (Fig. 4, left lane of each set) show extraction of intact DAT and 45- and 14-kDa fragments (Fig. 4, left arrows). When the immunizing peptide (peptide 16) was in-

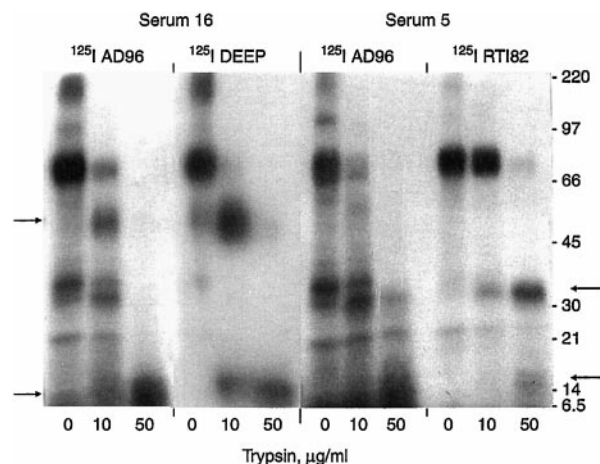


Fig. 3. Epitope-specific immunoprecipitation of [^{125}I]AD-96-129 proteolytic fragments. Rat striatal membranes labeled with [^{125}I]AD-96-129, [^{125}I]DEEP, or [^{125}I]RTI 82 were treated with the indicated concentrations of trypsin, followed by immunoprecipitation with antiserum 16 (left) or antiserum 5 (right). Samples were electrophoresed on 9 to 16% SDS-polyacrylamide gels followed by autoradiography. Arrows on the left indicate positions of 45- and 14-kDa fragments labeled with [^{125}I]AD-96-129 or [^{125}I]DEEP; arrows on the right indicate positions of 32- and 16-kDa fragments labeled with [^{125}I]AD-96-129 or [^{125}I]RTI 82.

cluded (Fig. 4, middle lanes) precipitation of these forms was blocked, whereas inclusion of an irrelevant peptide (peptide 5) had no effect (Fig. 4, right lanes). Precipitation of the 32-kDa band in the [125 I]AD-96-129 sample was not effectively blocked by peptide 16, again indicating its nonspecificity. In Fig. 4, right, tryptic digests of DATs labeled with [125 I]AD-96-129 or [125 I]RTI 82 and precipitated with serum 5 (Fig. 4, left lanes of each set) show extraction of intact DAT and 32-kDa fragments as well as fragments of 16 and 10 kDa in the [125 I]AD-96-129-labeled sample (Fig. 4, right arrows). Digestion of [125 I]RTI 82-labeled samples with higher levels of trypsin also generates fragments of 16 kDa (Fig. 3) and 10 kDa (data not shown). For the serum 5-precipitated samples inclusion of peptide 5 blocked precipitation of all forms (middle lanes), whereas inclusion of peptide 16 had no effect (right lanes). In conjunction with experiments showing that preimmune antiserum does not precipitate [125 I]AD-96-129-labeled intact DAT (Dutta et al., 2001b) or DAT fragments (data not shown), these results strongly confirm the specificity of immunorecognition of [125 I]AD-96-129-labeled fragments by antisera 16 and 5.

The pharmacological specificity of [125 I]AD-96-129 photo-incorporation into DAT and DAT proteolytic fragments is shown in Fig. 5. Inclusion of 10 μ M (–) cocaine during photolabeling of striatal membranes with [125 I]AD-96-129 inhibited labeling of DAT at 80 kDa (Fig. 5A, arrow) but not the labeling of several other proteins. The strongly labeled bands at 32 kDa may be the source of the 32-kDa contaminants present in some experiments. Figure 5B shows the serum 16 and serum 5 immunoprecipitation of tryptic fragments prepared from membranes labeled with [125 I]AD-96-129 in the presence and absence of cocaine. In addition to the displacement of the full-length bands (Fig. 5B, upper arrows) this figure shows the displacement of the 45-kDa band immunoprecipitated with serum 16 and the 32-kDa band immunoprecipitated with serum 5 (Fig. 5B, lower arrows). A small amount of radioactivity in both samples at 32 kDa that is not

displaced by cocaine may represent carryover of the nondisplaced 32-kDa protein during the extraction. Nevertheless, the substantial inhibition of [125 I]AD-96-129 labeling of these fragments by cocaine demonstrates that the incorporation of [125 I]AD-96-129 into both of these protein domains occurs with appropriate DAT pharmacological specificity. Additional pharmacological characterization of [125 I]AD-96-129 labeling is presented elsewhere (Dutta et al., 2001b).

The similarities in size and immunorecognition properties of the fragments labeled with [125 I]AD-96-129 to those of [125 I]DEEP and [125 I]RTI 82 indicate that [125 I]AD-96-129 is concomitantly incorporated in the same regions of the DAT primary sequence as these ligands. Previous characterization of [125 I]DEEP-labeled tryptic fragments showed that the 45-kDa band is a glycosylated fragment containing the N-terminal half of the protein beginning at or near the N terminus and extending through a site in EL2, whereas the 14-kDa band is a nonglycosylated product of this fragment containing TMs 1 to 2 but not TM3. Further proteolysis generates a 4-kDa fragment that does not contain epitope 16 and cannot be immunoprecipitated (Vaughan, 1995; Vaughan and Kuhar, 1996). Characterization of [125 I]RTI 82 fragments showed they are not glycosylated, and that the 32-kDa fragment begins N terminally at a site in EL2 and extends through most or all of the C-terminal tail, whereas the 16-kDa band is a product of this fragment beginning in EL2 and extending through TM7. The initial proteolytic cut that generates the 45- and 32-kDa fragments occurs on the C-terminal side of EL2, because it separates glycosylation sites on

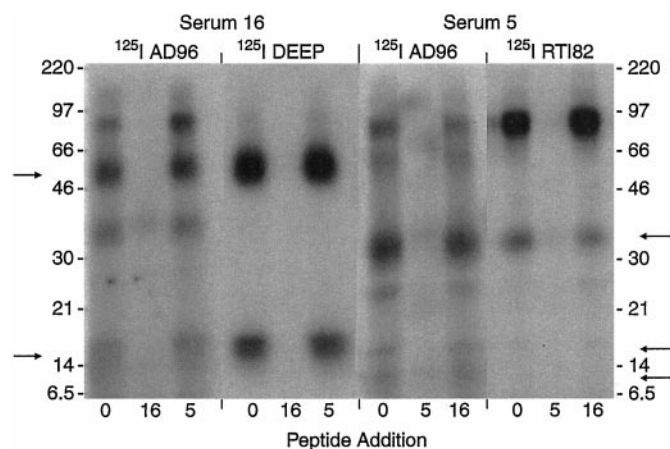


Fig. 4. Specificity of photoaffinity-labeled fragment immunoprecipitation. Rat striatal membranes labeled with [125 I]AD-96-129, [125 I]DEEP, or [125 I]RTI 82 were treated with 10 μ g/ml trypsin followed by immunoprecipitation with serum 16 (left) or serum 5 (right). During precipitation samples received either no addition, 50 μ g/ml peptide 16, or 50 μ g/ml peptide 5, as indicated. Arrows on the left indicate position of 45- and 14-kDa fragments labeled with [125 I]AD-96-129 or [125 I]DEEP, arrows on the right indicate positions of 32-, 16-, and 10-kDa fragments labeled with [125 I]AD-96-129 or [125 I]RTI 82. Note the slightly different migration patterns of the standards for the two panels.

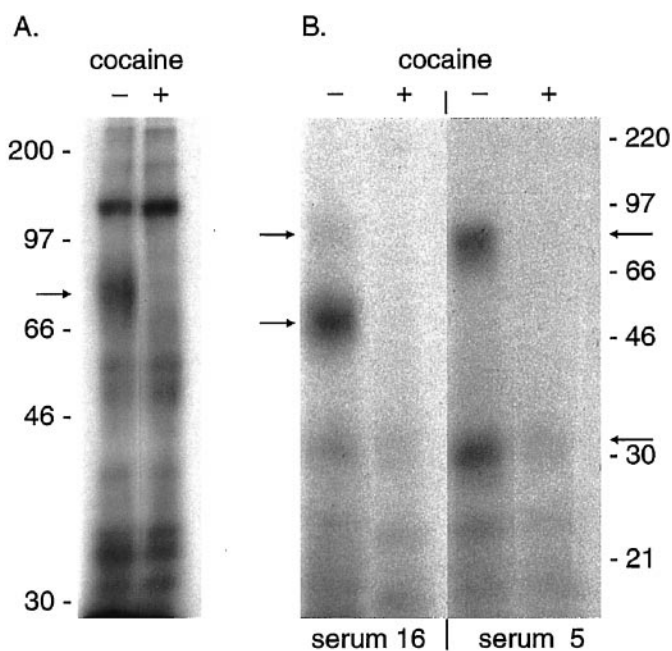


Fig. 5. Pharmacological specificity of [125 I]AD-96-129 labeling of DAT and DAT tryptic fragments. Striatal membranes were labeled with [125 I]AD-96-129 in the absence or presence of 10 μ M (–) cocaine as indicated. A, labeled membranes were electrophoresed directly on an 8% gel followed by electrophoresis and autoradiography. The arrow shows the position of full-length DAT at 80 kDa. B, [125 I]AD-96-129-labeled membranes were treated with 50 μ g/ml trypsin followed by immunoprecipitation with serum 16 or serum 5, electrophoresis on a 9 to 16% gel, and autoradiography. The arrows on the left show the positions of the intact DAT and the 45-kDa fragment precipitated with serum 16, the arrows on the right show the position of intact DAT and the 32-kDa fragment precipitated with serum 5.

the 45-kDa fragment from the serum 5 epitope on the 32-kDa fragment (Vaughan and Kuhar, 1996). The most likely site of this protease cut is R218, which is the only potential tryptic site between the *N*-glycosylation sites and epitope 5 (Fig. 6, arrow), or R227, which is within epitope 5, but might leave enough of the epitope to allow fragment precipitation. Figure 6 summarizes the results obtained for fragments labeled with [¹²⁵I]AD-96-129 and their relationship to incorporation sites of the other photoaffinity labels we have examined.

The isolation of 10-kDa [¹²⁵I]AD-96-129 and [¹²⁵I]RTI 82-labeled fragments with serum 5 may provide evidence that the incorporation of these ligands occurs within ~90 residues of the EL2 protease site at R218 or R227. The potential trypsin sites that best fit this estimate are R294 and R303 in EL3 between TMs 5 and 6, which would generate fragments of calculated molecular mass of 8 to 9 kDa, and K336, and R343 in intracellular loop 3 between TMs 6 and 7, which would generate fragments of calculated molecular mass of 13 to 14 kDa. The more conservative estimate indicating [¹²⁵I]RTI 82 and [¹²⁵I]AD-96-129 incorporation between EL2 to intracellular loops 3 (TMs 4–6) is shown in Fig. 6.

The relative amount of [¹²⁵I]AD-96-129 incorporation into the TM1 to 2 and TM4 to 6 domains was estimated from the intensities of the 45- and 32-kDa fragments in the overall peptide maps in Fig. 2, and by comparing the intensities of the 45- or 32-kDa fragments to those of the full-length DAT precipitated by each antiserum in Figs. 3 and 4. Densitometric quantitation of these experiments indicates that ligand distribution was approximately 33% in the TM1 to 2 region and 67% in the TM4 to 6 region.

Protease Sensitivity. In previous studies we observed that DATs labeled with [¹²⁵I]DEEP or [¹²⁵I]RTI 82 displayed a pronounced difference in protease sensitivity, with [¹²⁵I]DEEP-labeled DATs being readily proteolyzed, whereas those labeled with [¹²⁵I]RTI 82 were markedly protease resistant (Vaughan, 1995; Vaughan and Kuhar, 1996). Because the initial tryptic proteolysis site that cuts the protein into the 45- and 32-kDa fragments is on the C-terminal side of EL2 near TM4, we speculated that [¹²⁵I]RTI 82 incorporation in the TM4 to 6 region may be occurring close to the protease

site, obscuring its availability for proteolysis and resulting in protease resistance, whereas the incorporation of [¹²⁵I]DEEP in TMs 1 to 2, which may be more distant from the protease site, does not affect its availability and leaves the protein susceptible to proteolysis. We noted during characterization of [¹²⁵I]AD-96-129 binding that DATs labeled with this compound displayed a protease sensitivity intermediate to those of DATs labeled with [¹²⁵I]DEEP or [¹²⁵I]RTI 82. In Fig. 4, for example, after treatment with 10 μg/ml trypsin, the amount of full-length (unproteolyzed) DAT remaining relative to that of the 45- or 32-kDa fragments is very low for DATs labeled with [¹²⁵I]DEEP, is high for DATs labeled with [¹²⁵I]RTI 82, and is intermediate for DATs labeled with [¹²⁵I]AD-96-129. A comparable trend is evident in Fig. 3.

To characterize this more fully, we performed a more detailed trypsin dose-response analysis for samples labeled with all three ligands and determined the relative extent of proteolysis by monitoring the amount of full-length DATs remaining after treatment (Fig. 7). DATs labeled with [¹²⁵I]DEEP display their typical protease sensitivity with 3 to 10 μg/ml trypsin producing 80 to 95% loss of full-length forms, whereas DATs labeled with [¹²⁵I]RTI 82 show only 20 to 50% degradation at those doses. In two independent experiments we found that samples labeled with [¹²⁵I]AD-96-129 displayed a protease sensitivity intermediate between these two at all trypsin concentrations tested. This is evident in the autoradiograph (Fig. 7A) and is summarized quantitatively in Fig. 7B. These results indicate a correlation between the extent of ligand incorporation in the TM4 to 6

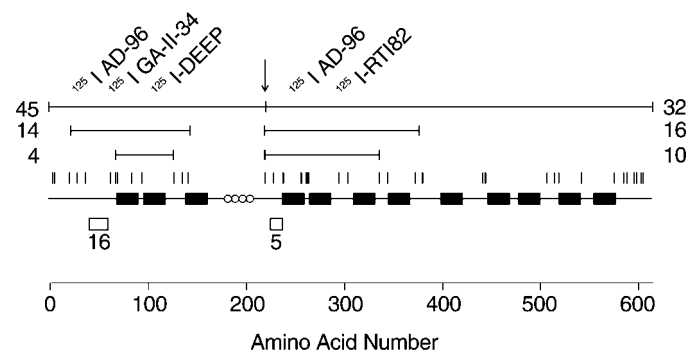


Fig. 6. Summary of DAT photoaffinity ligand binding sites. Schematic diagram of rat dopamine transporter primary amino acid sequence, with transmembrane domains indicated by filled rectangles; antibody 16 and 5 epitopes shown by open, numbered rectangles; consensus *N*-glycosylation sites indicated by open circles; and lysine and arginine residues (potential trypsin proteolysis sites) shown by tic marks. The arrow indicates the position of the initial tryptic proteolysis site at R218. The bars above the protein sequence represent the major photoaffinity-labeled fragments identified in these studies, with the mass of each fragment indicated to the left or right. The ligands that become incorporated in the fragments are indicated above the bars.

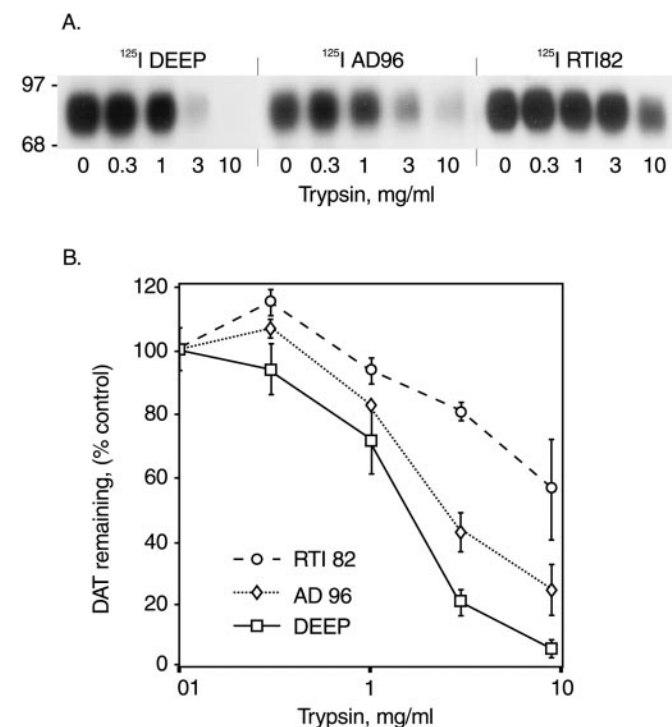


Fig. 7. Differential protease sensitivity of photoaffinity labeled DATs. A, rat striatal membranes labeled with [¹²⁵I]AD-96-129, [¹²⁵I]DEEP, or [¹²⁵I]RTI 82 were treated with the indicated concentrations of trypsin followed by immunoprecipitation with serum 16, electrophoresis, and autoradiography. B, densitometric quantitation of full-length DAT from each of the photolabeled samples, expressed as amount of photoaffinity-labeled protein remaining relative to untreated control samples. Values shown are the average of two experiments, error bars indicate standard deviation.

domain and the degree of resistance to proteolysis at the tryptic site in EL2. Inclusion of 1 μ M RTI 82 or AD-96-129 during trypsin treatment of [125 I]DEEP-labeled samples did not affect the DAT protease sensitivity, indicating that the resistance of the [125 I]RTI 82 and [125 I]AD-96-129 samples to proteolysis was not due to inhibition of trypsin activity by residual uncomplexed radioligand in those samples.

Discussion

Potential Proximity of Labeled Domains. This study documents the incorporation of a novel dopamine transporter photoaffinity ligand, [125 I]AD-96-129, into two distinct regions of the DAT primary sequence. These regions encompass TMs 1 to 2 near the N terminus of the protein and TMs 4 to 6 in the central third of the protein, both of which are major sites of incorporation for three other DAT photoaffinity ligands, [125 I]DEEP, [125 I]RTI 82, and [125 I]GA II 34. Previous studies have shown that [125 I]DEEP and [125 I]GA II 34 become incorporated primarily in the TM1 to 2 site, whereas [125 I]RTI 82 and a very slight amount of [125 I]DEEP become incorporated in the TM 4 to 6 region. In contrast to the specific or near-specific incorporation of these photolabels into one or the other region, [125 I]AD-96-129 incorporation occurred at comparable levels in both sites at a concentration (5 nM) well below its IC_{50} value of 154 nM for inhibiting binding of the cocaine analog [3 H]WIN 35,428 (Dutta et al., 2001b). These results strongly suggest that these regions are in spatial proximity and argue against the possibility that one of the domains represents a spatially distinct low-affinity site. Dual incorporation of photoaffinity labels in distinct regions of the primary sequence on VMAT (Sievert and Ruoho, 1997) and the multidrug resistance transporter, P-glycoprotein (Bruggemann et al., 1992; Greenberger 1993; Dey et al., 1997) has also been taken as evidence for the three-dimensional proximity of the labeled domains. Interestingly, one of the labeling sites on VMAT is near TM1, indicating a potential similarity to the DAT TM 1 to 2 site. Dual incorporation of [125 I]AD-96-129 may also represent ligand interaction with different transport cycle states of DAT. A similar conclusion has recently been obtained for the two photolabel sites on P-glycoprotein, but the labeled domains are nevertheless thought to be in proximity (Dey et al., 1997).

Because the incorporation of all DAT photoaffinity ligands determined to date has been associated with one or both of these sites, the current evidence implicating the proximity of these domains presents the possibility that these regions may contain binding determinants common to multiple uptake blockers. It is possible that these ligands are accommodated within a similar, although not necessarily identical, binding pocket, and their different sites of incorporation result from their particular spatial orientations within that site. This is indicated schematically in Fig. 8, which shows a binding pocket generated at least partially by TMs 1 to 2 and 4 to 6, and types of ligand orientations within that pocket that could generate the three patterns of photoincorporation we have observed. We do not know the specific site of ligand attachment within these domains, and have modeled incorporation of [125 I]AD-96-129 and [125 I]DEEP to occur in TM1 due to the evidence implicating TM1 in transport, antagonist binding, and photoaffinity labeling of DAT, SERT, and

VMAT (Kitayama et al., 1992; Sievert and Ruoho 1997; Barker et al., 1998, 1999), whereas incorporation of [125 I]RTI 82 and [125 I]AD-96-129 was modeled in TM4 to place them close to the EL2 protease site that is affected by ligand incorporation in the TM 4 to 6 domain. Future studies will be aimed at directly identifying additional binding domains for these compounds by developing ligands with the azido moiety placed in different positions, as well as more precisely determining the incorporation sites of existing compounds. The recent indications of SERT multimers also presents the possibility that the ligand binding pocket on monoamine transporters may be composed of these regions on different polypeptides (Kilic and Rudnick, 2000).

The juxtaposition of TMs 1 to 2 and 4 to 6 to form part of a binding pocket for multiple classes of uptake blockers is compatible with observations from several other studies on determinants for transport and antagonist binding at DAT, NET, and SERT, many of which indicate involvement of residues and domains in diverse regions of the primary sequence. Sites proposed to function in binding of cocaine or cocaine analogs in DAT include D79 in TM1 (Kitayama et al., 1992) and various phenylalanine and proline residues in TMs 1, 2, 5, and 7 (Lin et al., 1999, 2000); valine and isoleucine residues in TM3 of DAT, NET, and SERT (Chen et al., 1997; Chen and Rudnick, 2000; Lee et al., 2000), and a TM 5 to 8 domain in DAT-NET chimeras (Giros et al., 1994). In addition, cocaine inhibits the accessibility of DAT residue C90 to sulfhydryl reagents, implicating cocaine-induced conformational changes in TMs 1 to 2 (Ferrer and Javitch, 1998). In our proposed binding pocket the N_3 group of [125 I]RTI 82 is oriented for attachment in TM 4 to 6, whereas other aspects of the molecule may retain the potential for reversible interactions with residues in TMs 1 to 3 and/or additional sites in TMs 5 to 8. Although less is known about binding of GBR compounds, studies performed with DAT/NET chimeras indicated that TMs 5 to 8 and 1 to 3 contribute primary and

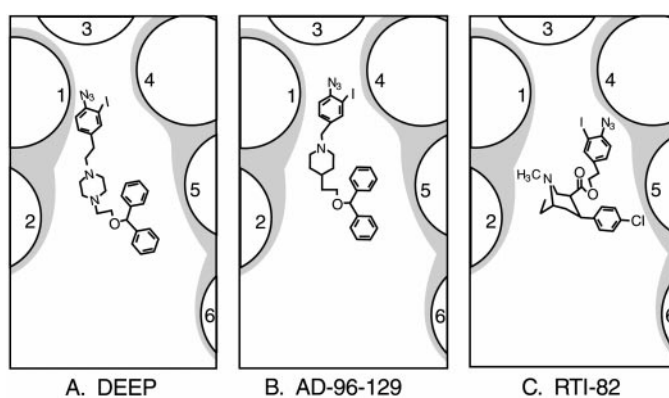


Fig. 8. Model of photoaffinity label binding to DAT. Schematic cross-sectional view of a section of DAT shown from the extracellular side of the membrane. Transmembrane spanning helices are indicated as numbered circles and are primarily arranged in the clockwise order suggested to provide favorable helix packing (Edwardsen and Dahl, 1994); interhelical connecting loops are not shown. Shading indicates the photoaffinity-labeled domains identified in these studies. A–C, hypothetical orientation of DEEP, AD-96-129, and RTI 82 for N_3 group incorporation in the TM 1 to 2 domain (A), the TM 4 to 6 domain (C), or either domain (B). DEEP and AD-96-129 are modeled as having substantial similarity in their binding site orientations. The positioning of other aspects of the ligands with relative to the protein is not known and as shown is arbitrary. Incorporation of ligands was modeled to occur in TMs 1 and 4 of the possible helices in each shaded domain (see text for details).

secondary affinity sites, respectively, for GBR binding (Buck and Amara, 1995). Our model is compatible with interaction of the GBR-like derivatives [125 I]DEEP and [125 I]AD-96-129 with both of these domains, showing direct interaction of the phenyl-azido group with TMs 1 to 2, whereas other parts of the molecule, including the diphenyl moiety essential for high-affinity GBR binding (Dutta et al., 2001a), retains the potential for orientation with other regions such as the TM 5 to 8 primary affinity site. The juxtaposition of the TM 1 to 2 and TM 4 to 6 photolabeled domains may also be consistent with proximity of residues in EL2 and TMs 7 to 8 induced by binding of zinc (Loland et al., 1999).

Molecular Determinants of Ligands. The incorporation profiles of the four irreversible ligands we have examined may begin to elucidate the structural determinants that contribute to and affect their binding. All of the compounds that label the TM 1 to 2 domain, [125 I]DEEP, [125 I]AD-96-129, and [125 I]GA II 34, contain a diphenyl moiety, indicating the potential for these ring structures to orient the ligands similarly within the binding pocket, possibly via π - π interactions with aromatic groups on the protein. Molecular differences that may produce greater association of [125 I]AD-96-129 than [125 I]DEEP with the TM 4 to 6 domain include the 125 I-AD-96-129 piperidine ring. The N-atom in this group has a different pK_a than the piperazine N-atoms in [125 I]DEEP, which may result in different hydrogen or ionic bonding interactions with the protein. Another difference between [125 I]DEEP and [125 I]AD-96-129 is the length of the aromatic-alkyl chain connecting to the N-atom of the piperidine or piperazine ring, which may give rise to differential steric properties or ligand flexibilities. It is intriguing that dual incorporation, albeit to different extents, is seen for the GBR-like compounds [125 I]DEEP and [125 I]AD-96-129, whereas no evidence for multisite incorporation has been found for the tropane ring-containing compounds [125 I]RTI 82 and [125 I]GA II 34. It may be that conformational flexibility of GBR-like compounds allows ligand bending or movement within the binding pocket that promotes multisite incorporation. Cocaine and WIN compounds display substantial structural constraints imposed by the tropane ring (Zhu et al., 1999), which may minimize ligand movement and lead to the more discrete incorporation observed for [125 I]RTI 82 and [125 I]GA II 34. Future studies involving closely related structural variants of these ligands will help to further elucidate these issues.

Protease Sensitivity Effects of Ligands. Our finding that DATs labeled with different ligands display widely different protease sensitivities may be an indication of the existence of different structural states of ligand-complexed protein. These protease sensitivity studies were performed with native preparations of DAT, compatible with the results reflecting authentic variations in protein structure. Two possible scenarios may explain the finding that protease resistance is correlated with the extent of ligand incorporation in the TM 4 to 6 region. In one scenario, ligands that become incorporated in TMs 4 to 6 sterically cover the EL2 protease site and interfere with protease access, whereas ligands incorporated in TMs 1 to 2 are not near the site and leave the protein susceptible to proteolysis. This would imply a region of ligand-protein proximity along the C-terminal side of EL2 for some but not all ligands, and if ligand binding occurs within a membrane-embedded pocket as is conventionally

thought, would also imply that this region of EL2 would be situated close to the lipid bilayer. An alternative scenario is that ligand incorporation in TMs 4 to 6 induces a conformational change in the protein that results in the EL2 protease site becoming inaccessible to enzyme, or conversely that ligand incorporation in TM 1 to 2 promotes a conformation in which the protease site becomes more accessible. In either case, site-specific ligand incorporation produces different conformational changes, indicating that different blockers induce different conformational states of the protein. These results may suggest a relationship between conformational movements in EL2 and transport inhibition, and suggest that differences in the response of the protein to different blockers may be related to the subtle differences in DAT response observed for cocaine and GBR analogs. Stabilization of EL2 may also underlie the zinc-induced inhibition of dopamine transport (Loland et al., 1999).

Summary. This study provides the first direct evidence that distinct domains of DAT can interact with a single ligand, thus implicating the proximity of the irreversibly labeled domains to other regions that may contain additional binding determinants. This advances our understanding of the structure of ligand binding sites, which are likely to consist of residues that are far apart in primary sequence but close together three dimensionally. Although a computer model based on primary sequence has been developed for DAT (Edvardsen and Dahl, 1994), a three-dimensional structure based on NMR or crystallization is currently not available. The results shown here therefore contribute to a framework for understanding the structural basis of neurotransmitter transporter function.

References

- Barker EL, Moore KR, Rakhshan F and Blakely RD (1999) Transmembrane domain I contributes to the permeation pathway for serotonin and ions in the serotonin transporter. *J Neurosci* **19**:4705–4717.
- Barker EL, Perlman MA, Adkins EM, Houliha WJ, Pristupa ZB, Niznik HB and Blakely RD (1998) High affinity recognition of serotonin transporter antagonists defined by species-scanning mutagenesis. *J Biol Chem* **273**:19459–19468.
- Bruggemann EP, Currier SJ, Gottesman MM and Pastan I (1992) Characterization of the azidopine and vinblastine binding site of P-glycoprotein. *J Biol Chem* **267**:21020–21026.
- Buck K and Amara SG (1994) Chimeric dopamine-norepinephrine transporters delineate structural domains influencing selectivity for catecholamines and 1-methyl-4-phenylpyridinium. *Proc Natl Acad Sci USA* **91**:12584–12588.
- Buck K and Amara SG (1995) Structural domains of catecholamine transporter chimeras involved in selective inhibition by antidepressants and psychomotor stimulants. *Mol Pharmacol* **48**:1030–1037.
- Carroll FI, Lewin AH, Boja JW and Kuhar MJ (1992) Cocaine receptor: biochemical characterization and structure-activity relationship of cocaine analogues at the dopamine transporter. *J Med Chem* **35**:969–981.
- Chen J-G and Rudnick G (2000) Permeation and gating residues in serotonin transporter. *Proc Natl Acad Sci USA* **97**:1044–1049.
- Chen J-G, Sachatzidis A and Rudnick G (1997) The third transmembrane domain of the serotonin transporter contains residues associated with substrate and cocaine binding. *J Biol Chem* **272**:28321–28327.
- Dey S, Ramachandra M, Pastan I, Gottesman MM and Ambudkar SV (1997) Evidence for two non-identical drug-interaction sites in the human P-glycoprotein. *Proc Natl Acad Sci USA* **94**:10594–10599.
- Dutta AK, Coffey LL and Reith MEA (1997) Highly selective, novel analogs of 4-[2-(diphenylmethoxy)ethyl]-1-benzylpiperidine for the dopamine transporter: effect of different aromatic substitutions on their affinity and selectivity. *J Med Chem* **40**:35–43.
- Dutta AK, Coffey LL and Reith MEA (1998a) Potent and selective ligands for the dopamine transporter (DAT): structure-activity relationship studies of novel 4-[2-(diphenylmethoxy)ethyl]-1-(3-phenylpropyl)piperidine analogues. *J Med Chem* **41**:699–705.
- Dutta AK, Fei X-S, Beardsley PM and Reith MEA (2001a) Structure-activity relationship studies of 4-[2-(diphenylmethoxy)ethyl]-1-benzylpiperidine derivatives and their N-analogs: evaluation of behavioral activity of O- and N-analogs and their binding to monoamine transporters. *J Med Chem* **44**:937–948.
- Dutta A, Fei X-S, Vaughan RA, Gaffaney JD, Wang N, Lever J. and Reith MEA (2001b) Design, synthesis and characterization of 4-[2-(diphenylmethoxy)ethyl]-1-benzyl piperidine, a novel dopamine transporter photoaffinity label. *Life Sci* **68**:1839–1849.

- Dutta AK, Xu C and Reith MEA (1996) Structure-activity relationship studies of novel 4-[2-[bis(4-fluorophenyl)methoxy]ethyl]-1-(3-phenylpropyl)piperidine analogs: synthesis and biological evaluation at the dopamine and serotonin transporter sites. *J Med Chem* **39**:749–756.
- Dutta AK, Xu C and Reith MEA (1998b) Tolerance in the replacement of the benzhydrylic O-atom in 4-[2-(diphenyl-methoxy)ethyl]-1-benzylpiperidine derivatives by an N-atom: development of new-generation potent and selective N-analog molecules for the dopamine transporter. *J Med Chem* **41**:3293–3297.
- Edvardsen O and Dahl SG (1994) A putative model of the dopamine transporter. *Mol Brain Res* **27**:265–274.
- Ferrer JV and Javitch JA (1998) cocaine alters the accessibility of endogenous cysteines in putative extracellular and intracellular loops of the human dopamine transporter. *Proc Natl Acad Sci USA* **95**:9238–9243.
- Giros B, Wang Y-M, Suter S, McLeskey SB, Pifl C and Caron MG (1994) Delineation of discrete domains for substrate, cocaine, and tricyclic antidepressant interactions using chimeric dopamine-norepinephrine transporters. *J Biol Chem* **269**:15985–15988.
- Greenberger LM (1993) Major photoaffinity drug labeling sites for iodoaryl azidoprazosin in P-glycoprotein are within, or immediately C-terminal to, transmembrane domains 6 and 12. *J Biol Chem* **268**:11417–11425.
- Izenwasser S, Terry P, Heller B, Witkin JM and Katz JL (1994) Differential relationships among dopamine transporter affinities and stimulant potencies of various uptake inhibitors. *Eur J Pharmacol* **263**:277–283.
- Kilic F and Rudnick G (2000) Oligomerization of serotonin transporter and its functional consequences. *Proc Natl Acad Sci USA* **97**:3106–3111.
- Kinemuchi H, Fowler CJ and Tipton KF (1987) The neurotoxicity of 1-methyl-4-phenyl-1,2,3,6-tetrahydropyridine (MPTP) and its relevance to Parkinson's disease. *Neurochem Int* **11**:359–373.
- Kitayama S, Shimada S, Xu H, Markham L, Donovan D and Uhl GR (1992) Dopamine transporter site-directed mutations differentially alter substrate transport and cocaine binding. *Proc Natl Acad Sci USA* **89**:7782–7785.
- Kuhar MJ, Ritz MC and Boja JW (1991) The dopamine hypothesis of the reinforcing properties of cocaine. *Trends Neurosci* **14**:299–302.
- Lee S-H, Chang M-Y, Lee K-H, Park BS, Chin HR and Lee Y-S (2000) Importance of valine at position 152 for the substrate transport and 2 β -carbomethoxy-3 β -(4-fluorophenyl) tropane binding of dopamine transporter. *Mol Pharmacol* **57**:883–889.
- Lever JR, Carroll FI, Patel A, Abraham P, Boja J, Lewin A and Lew RJ (1993) Radiosynthesis of a photoaffinity probe for the cocaine receptor of the dopamine transporter: 3 β -(p-chlorophenyl)tropane-2 β -carboxylic acid m-([¹²⁵I]-iodo)-p-azidophenethyl ester ([¹²⁵I]-RTI-82). *J Label Compd Radiopharm* **33**:1131–1137.
- Lin Z, Itokawa M and Uhl GR (2000) Dopamine transporter proline mutations influence dopamine uptake, cocaine analog recognition and expression. *FASEB J* **14**:715–728.
- Lin Z, Wang W, Kopajtic T, Revay RS and Uhl GR (1999) Dopamine transporter transmembrane phenylalanine mutations can selectively influence dopamine uptake and cocaine analog recognition. *Mol Pharmacol* **56**:434–447.
- Loland CJ, Norregaard L and Gether U (1999) Defining proximity relationships in the tertiary structure of the dopamine transporter. *J Biol Chem* **274**:36928–36934.
- Madras BK, Spealman RD, Fahey MA, Neumeyer JL, Saha JK and Milius RA (1989) Cocaine receptors labeled by [³H]2 β -carbomethoxy-3 β -(4-fluorophenyl)tropane. *Mol Pharmacol* **36**:518–524.
- Mash DC and Staley JK (1997) The dopamine transporter in human brain. Characterization and effect of cocaine exposure, in *Neurotransmitter Transporters: Structure, Function, and Regulation* (Reith MEA ed) pp 315–343, Humana Press, Totowa, NJ.
- Povlock S and Amara S (1997) The structure and function of norepinephrine, dopamine, and serotonin transporters, in *Neurotransmitter Transporters: Structure, Function, and Regulation* (Reith MEA ed) pp 1–28, Humana Press, Totowa, NJ.
- Pristupa ZB, Wilson JM, Hoffman BJ, Kish SJ and Niznik HB (1994) Pharmacological heterogeneity of the cloned and native human dopamine transporter: disassociation of [³H]WIN 35,428 and [³H]GBR 12,935. *Mol Pharmacol* **45**:125–135.
- Rothman RB, Greig N, Kim A, DeCosta BR, Rice KD, Carroll FI and Pert A (1992) Cocaine and GBR 12909 produce equivalent motoric responses at different occupancy of the dopamine transporter. *Pharmacol Biochem Behav* **43**:1135–1142.
- Sievert MK and Ruoho AE (1997) Peptide mapping of the [¹²⁵I]iodoazidoketanserin and [¹²⁵I]2-N-[(3'-iodo-4'-azidophenyl)propionyl]tetrabenazine binding sites for the synaptic vesicle monoamine transporter. *J Biol Chem* **272**:26049–26055.
- Vaughan RA (1995) Photoaffinity-labeled ligand binding domains on dopamine transporters identified by peptide mapping. *Mol Pharmacol* **47**:956–964.
- Vaughan RA, Agoston GE, Lever JR and Newman AH (1999) Differential binding of tropane-based photoaffinity ligands on the dopamine transporter. *J Neurosci* **19**:630–636.
- Vaughan RA and Kuhar MJ (1996) Dopamine transporter ligand binding domains: structural and functional properties revealed by limited proteolysis. *J Biol Chem* **271**:21672–21680.
- Zhu N, Harrison A, Trudell ML and Klein-Stevens CL (1999) QSAR and CoMFA study of cocaine analogs: crystal and molecular structure of (–) cocaine hydrochloride and n-methyl-3 β -(p-fluorophenyl)tropane-2 β -carboxylic acid methyl ester. *Struct Chem* **10**:91–103.

Send reprint requests to: Dr. Roxanne Vaughan, Department of Biochemistry and Molecular Biology, University of North Dakota School of Medicine and Health Sciences, 501 N. Columbia Rd., Grand Forks, ND 58203-9037. E-mail: rvaughan@medicine.nodak.edu